Available online at www.sciencedirect.com
SCIENCE DIRECT®

ELSEVIER

Journal of Sound and Vibration 285 (2005) 407–424

JOURNAL OF SOUND AND VIBRATION

www.elsevier.com/locate/jsvi

Optimal design for passive suspension of a light rail vehicle using constrained multiobjective evolutionary search

Niahn-Chung Shieh[a], Chun-Liang Lin[b,*], Yu-Chen Lin[c], Kuo-Zoo Liang[d]

[a]*Chung Shan Institute of Science and Technology, Taoyuan 325, Taiwan, ROC*
[b]*Department of Electrical Engineering, National Chung Hsing University, 250 Kuo Kuang Road, Taichung 402, Taiwan, ROC*
[c]*Institute of Automatic Control Engineering, Feng Chia University, Taichung 407, Taiwan, ROC*
[d]*Department of Mechanical Engineering, Ching-Yun University, Chungli 320, Taiwan, ROC*

Received 28 August 2003; received in revised form 26 February 2004; accepted 26 August 2004
Available online 24 November 2004

Abstract

This research proposes a systematic and effective optimization process for the design of vertical passive suspension of light rail vehicles (LRVs) using new constrained multiobjective evolution algorithms. A multibody dynamic model of the three-car train set is presented and the suspension spring and damping parameters are optimally designed. A new design of the passive suspension is aided by the use of evolution algorithms to attain the best compromise between ride quality and suspension deflections due to irregular gradient tracks. Extensive simulations are performed to verify the proposed design scheme. The preliminary results show that, when the passive suspension is optimized via the proposed approach, a substantial improvement in the vertical ride quality is obtained while keeping the suspension deflections within their allowable clearance when the light rail vehicle runs onto the worst track condition.

1. Introduction

The major functions of suspension for light rail vehicles (LRVs) are to support the carbody and bogie, to isolate the forces generated by the track unevenness at the wheels, and to control the

*Corresponding author.
E-mail address: chunlin@dragon.nchu.edu.tw (C.-L. Lin).

doi:10.1016/j.jsv.2004.08.014

Nomenclature

- $S(\varphi)$ spatial power spectral density (PSD) of track vertical profile
- A_1 roughness constant of spatial power spectral density (4.5e–4 in^2 cpf)
- φ spatial frequency (cpf, cycle/ft)
- φ_1, φ_2 break frequencies of spatial power spectral density (0.0071 cpf, 0.04 cpf)
- ω circular frequency (rad/s)
- v nominal light rail vehicle velocity (70 km/h)
- y_1 vertical displacement of the centre of gravity (c.g.) position of first power-carbody (1 dof)
- y_2 vertical displacement of the c.g. position of trailer-carbody (2 dof)
- y_3 vertical displacement of the c.g. position of second power-carbody (3 dof)
- θ_1 pitch angle of the c.g. position of first power-carbody (4 dof)
- θ_2 pitch angle of the c.g. position of trailer-carbody (5 dof)
- θ_3 pitch angle of the c.g. position of second power-carbody (6 dof)
- y_4 vertical displacement of the c.g. position of first power-bogie (7 dof)
- y_5 vertical displacement of the c.g. position of trailer-bogie (8 dof)
- y_6 vertical displacement of the c.g. position of second power-bogie (9 dof)
- y_7 track vertical profile (track irregularity) for first power-bogie (base motion input)
- y_8 track vertical profile (track irregularity) for trailer-bogie (base motion input)
- y_9 track vertical profile (track irregularity) for second power-bogie (base motion input)
- y_{10} vertical displacement of the suspension position of first power-carbody
- y_{12} vertical displacement of the rear position of first power-carbody
- y_{13} vertical displacement of the front position of trailer-carbody (connecting first power-carbody)
- y_{24} vertical displacement of the rear position of trailer-carbody (connecting second power-carbody)
- y_{11} vertical displacement of the suspension position of second power-carbody
- y_{23} vertical displacement of the rear position of second power-carbody
- m_p power-carbody mass (10820 kg)
- I_p power-carbody pitch inertia (71000 kg m^2)
- m_t trailer-carbody mass (4470 kg)
- I_t trailer-carbody pitch inertia (6000 kg m^2)
- m_{pb} power-bogie mass (2940 kg)
- m_{tb} trailer-bogie mass (1150 kg)
- d_1 distance between c.g. and suspension positions of power-carbody (2.825 m)
- d_2 distance between c.g. and rear positions of power-carbody (6 m)
- d_3 distance between c.g. and end positions of trailer-carbody (1.9625 m)
- k_1, c_1 spring and damping constants of secondary suspension of power-carbody
- k_2, c_2 spring and damping constants of secondary suspension of trailer-carbody
- k_3, c_3 spring and damping constants of primary suspension of power-carbody
- k_4, c_4 spring and damping constants of primary suspension of trailer-carbody
- k spring constant of articulation (1630000 N/m)
- x, z state and output variables of dynamic system
- J_1, J_2, J_3 objective function of three vehicles

attitude of the carbody with respect to the track surface for providing ride comfort. Accordingly, the suspension influences vehicle ride comfort and stability, and should be designed to isolate the carbody from track roughness, and to maintain suitable space between the track and carbody.

In the past decades, only a limited number of papers have been focused on the optimal design of railway vehicle suspensions [1]. Recently, researchers have paid more attention to the investigation of problems of this kind [2–4]. In the traditional design approaches, suspension parameters are designed on the basis of the suspension's maximum stroke, static deflection and bouncing natural frequency of carbodies. In practice, the acceleration of carbodies and the total suspension deflection due to irregular gradient track must be considered simultaneously. However, it is usually a difficult objective to meet all conflicting objectives among ride comfort and suspension compactness. Finding suspension parameters to simultaneously satisfy all conflicting objectives is so complicated that it is difficult to solve analytically or even numerically. Fortunately, recent applications in genetic algorithms (GAs) [2,3,5] and evolution algorithms (EAs) [6–8] offer efficient ways to resolve the problem. EAs involving the parallel process are stochastic optimization algorithms, which work directly with the real representation of the parameter set searching from an initial population. Compared to the genetic algorithms (GAs) [9], EAs' transition rules are deterministic and the constraints are handled with the non-feasible individual eliminated. Because of the real representation of parameters the coding and decoding processes can be omitted. Considering many points in the search space, an EA has less chance of converging to the local optimum and is more likely to converge to the global one. This means that it can result in higher accurate solutions while solving for the optimization problems. In Ref. [10], a tutorial survey of recent works on penalty techniques used in general genetic algorithms was presented.

The simplest and most common type of suspensions are the passive systems, which use dampers and springs between the carbody and the bogie (i.e. secondary suspension), and between the bogie and the axles (i.e. primary suspension) to support the carbody and to isolate disturbances from the track to the carbody. In this study, a 9 degree of freedom (dof) multibody dynamic model of a three-car train set is developed and eight suspension spring and damping parameters under selection are optimized. An EA is used to achieve the best compromise between ride quality, primary and secondary suspension deflections due to irregular gradient track. Here we develop a new constrained multiobjective evolution algorithm to assist the suspension design and handle the unavoidable conflict between the ride quality and suspension deflection. The effectiveness of the proposed algorithm is verified with extensive computer simulations.

2. LRV configuration and track characteristics

The LRV considered is composed of two power-carbodies with two power-bogies (each equipped with two traction motors), one trailer-carbody with one trailer-bogie, as shown in Fig. 1. Each end carbody is connected with one power-bogie by the use of a bolster, while the middle carbody is directly connected with one bolsterless trailer-bogie. An articulation is used to connect the power-carbody and the trailer-carbody. The low floor area is about 70% of the total floor area. The track gauge is 1067 mm. The primary suspension consists of rubber chevrons and the secondary suspension comprises coil springs and dampers.

To design the passive railway suspensions, the response to the deterministic (the design alignment) and random inputs of the track (track irregularities) must be taken into account. Typical railway gradients are considered for checking the suspension deflections due to the

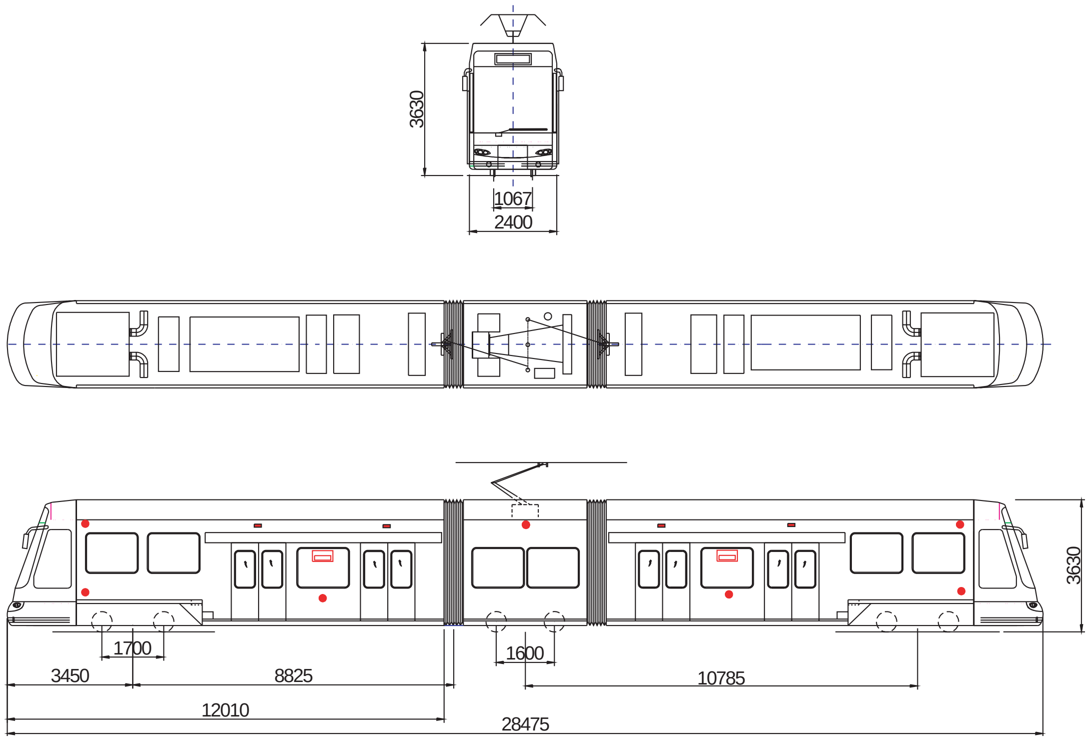

Fig. 1. Layout of the prototype for the presented LRV.

deterministic input of the track. In addition, the random track, representing the roughness of a typical line, is derived from a spatial power spectrum of the track vertical profile. The spatial power spectral density (PSD) of the track vertical profile can be expressed as [11]

$$S(\varphi) = \frac{A_1 \varphi_2^2 (\varphi^2 + \varphi_1^2)}{\varphi^4 (\varphi^2 + \varphi_2^2)}. \tag{1}$$

Using the relation $\varphi = f/v$ and $S(f) = S(\varphi)/v$, where v is the velocity of LRV, we can obtain the PSD of track vertical profile $S(f)$ [12].

3. LRV modelling

Due to symmetry, only a single side of the LRV model needs to be considered in the vertical direction; see Fig. 2. There are 2 dofs for each carbody associated with its bounce and pitch motions, and 1 dof for each bogie associated with its bounce motion. Consequently, a 9 dof dynamic model is built. The base motion input to the LRV is the track vertical profile and the track gradient, which takes the time delay into consideration. Another concern is the movements of the suspension mounting and the articulation (end) positions of the LRV, which may be represented as follows:

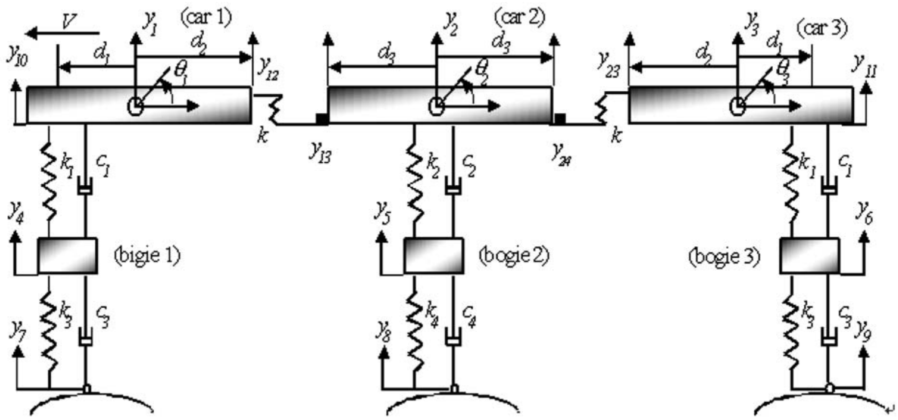

Fig. 2. Multibody dynamic model of LRV.

$$y_{10} = y_1 - d_1\theta_1, \quad y_{12} = y_1 + d_2\theta_1, \quad y_{13} = y_2 - d_3\theta_2,$$

$$y_{24} = y_2 + d_3\theta_2, \quad y_{23} = y_3 - d_2\theta_3, \quad y_{11} = y_3 + d_1\theta_3. \tag{2}$$

The force in the secondary suspension between the carbody and the bogie is due to the relative displacement of suspension mounting. In particular, the force in articulation between carbodies is due to the relative displacement of articulation. The articulation is modelled as a spring with vertical deflection capacity. Using the d'Alembert force method [13], the mathematical representation for the LRV is rigorously derived as follows:

$$m_p\ddot{y}_1 + c_1\dot{y}_1 - c_1d_1\dot{\theta}_1 - c_1\dot{y}_4 + (k_1+k)y_1 - ky_2 + (kd_2 - k_1d_1)\theta_1 + kd_3\theta_2 - k_1y_4 = 0,$$

$$m_t\ddot{y}_2 + c_2\dot{y}_2 - c_2\dot{y}_5 - ky_1 + (k_2+2k)y_2 - ky_3 - kd_2\theta_1 + kd_2\theta_3 - k_2y_5 = 0,$$

$$m_p\ddot{y}_3 + c_1\dot{y}_3 + c_1d_1\dot{\theta}_3 - c_1\dot{y}_6 - ky_2 + (k_1+k)y_3 - kd_3\theta_2 + (k_1d_1 - kd_2)\theta_3 - k_1y_6 = 0,$$

$$I_p\ddot{\theta}_1 - c_1d_1\dot{y}_1 + c_1d_1^2\dot{\theta}_1 + c_1d_1\dot{y}_4 + (kd_2 - k_1d_1)y_1 - kd_2y_2 + (k_1d_1^2 + kd_2^2)\theta_1 + kd_2d_3\theta_2 + k_1d_1y_4 = 0,$$

$$I_t\ddot{\theta}_2 + kd_3y_1 - kd_3y_3 + kd_2d_3\theta_1 + 2kd_3^2\theta_2 + kd_2d_3\theta_3 = 0,$$

$$I_p\ddot{\theta}_3 + c_1d_1\dot{y}_3 + c_1d_1^2\dot{\theta}_3 - c_1d_1\dot{y}_6 + kd_2y_2 + (k_1d_1 - kd_2)y_3 + kd_2d_3\theta_2 + (k_1d_1^2 + kd_2^2)\theta_3 - k_1d_1y_6 = 0,$$

$$m_{\mathrm{pb}}\ddot{y}_4 - c_1\dot{y}_1 + c_1d_1\dot{\theta}_1 + (c_1+c_3)\dot{y}_4 - k_1y_1 + k_1d_1\theta_1 + (k_1+k_3)y_4 = k_3y_7 + c_3\dot{y}_7,$$

$$m_{\mathrm{tb}}\ddot{y}_5 - c_2\dot{y}_2 + (c_2+c_4)\dot{y}_5 - k_2y_2 + (k_2+k_4)y_5 = k_4y_8 + c_4\dot{y}_8,$$

$$m_{\mathrm{pb}}\ddot{y}_6 - c_1\dot{y}_3 - c_1d_1\dot{\theta}_3 + (c_1+c_3)\dot{y}_6 - k_1y_3 - k_1d_1\theta_3 + (k_1+k_3)y_6 = k_3y_9 + c_3\dot{y}_9, \tag{3}$$

where $m_i\ddot{y}_j(I_i\ddot{\theta}_j)$, $c_i\dot{y}_j$ ($c_id_j\dot{y}_k, c_id_j\dot{\theta}_k$ and $c_id_j^2\dot{\theta}_k$) and k_iy_j ($k_id_jy_k, k_id_j\theta_k$ and $k_id_j^2\theta_k$) are the inertia force, damping force and spring force, respectively. The main outputs of interest from the vehicle are the body accelerations at various measurement positions and the suspension deflections.

The set of equations of motion can be lumped into a second-order matrix equation:

$$[M]\{\ddot{q}\} + [C]\{\dot{q}\} + [K]\{q\} = \{r\}, \tag{4}$$

where the generalized coordinates vector $q = [y_1y_2y_3\theta_1\theta_2\theta_3y_4y_5y_6]^{\mathrm{T}}$, the inertia matrix, the damping matrix, and the stiffness matrix, and $r \in \Re^9$ are, respectively, defined as follows:

$$M = \mathrm{diag}(m_p, m_t, m_p, I_p, I_t, I_p, m_{\mathrm{pb}}, m_{\mathrm{tb}}, m_{\mathrm{pb}}),$$

$$C = \begin{bmatrix} c_1 & 0 & 0 & -c_1d_1 & 0 & 0 & -c_1 & 0 & 0 \\ 0 & c_2 & 0 & 0 & 0 & 0 & 0 & -c_2 & 0 \\ 0 & 0 & c_1 & 0 & 0 & c_1d_1 & 0 & 0 & -c_1 \\ -c_1d_1 & 0 & 0 & c_1d_1^2 & 0 & 0 & c_1d_1 & 0 & 0 \\ 0 & 0 & 0 & 0 & 0 & 0 & 0 & 0 & 0 \\ 0 & 0 & c_1d_1 & 0 & 0 & c_1d_1^2 & 0 & 0 & -c_1d_1 \\ -c_1 & 0 & 0 & c_1d_1 & 0 & 0 & c_1+c_3 & 0 & 0 \\ 0 & -c_2 & 0 & 0 & 0 & 0 & 0 & c_2+c_4 & 0 \\ 0 & 0 & -c_1 & 0 & 0 & -c_1d_1 & 0 & 0 & c_1+c_3 \end{bmatrix},$$

$$K = \begin{bmatrix} k+k_1 & -k & 0 & -k_1d_1+kd_2 & kd_3 & 0 & -k_1 & 0 & 0 \\ -k & k_2+2k & -k & -kd_2 & 0 & kd_2 & 0 & -k_2 & 0 \\ 0 & -k & k_1+k & 0 & -kd_3 & k_1d_1-kd_2 & 0 & 0 & -k_1 \\ -k_1d_1+kd_2 & -kd_2 & 0 & k_1d_1^2+kd_2^2 & kd_2d_3 & 0 & k_1d_1 & 0 & 0 \\ kd_3 & 0 & -kd_3 & kd_2d_3 & 2kd_3^2 & kd_2d_3 & 0 & 0 & 0 \\ 0 & kd_2 & k_1d_1-kd_2 & 0 & kd_2d_3 & k_1d_1^2+kd_2^2 & 0 & 0 & -k_1d_1 \\ -k_1 & 0 & 0 & k_1d_1 & 0 & 0 & k_1+k_3 & 0 & 0 \\ 0 & -k_2 & 0 & 0 & 0 & 0 & 0 & k_2+k_4 & 0 \\ 0 & 0 & -k_1 & 0 & 0 & -k_1d_1 & 0 & 0 & k_1+k_3 \end{bmatrix},$$

$$r = [0 \;\; 0 \;\; 0 \;\; 0 \;\; 0 \;\; 0 \;\; k_3y_7 + c_3\dot{y}_7 \;\; k_4y_8 + c_4\dot{y}_8 \;\; k_3y_9 + c_3\dot{y}_9]^{\mathrm{T}}$$

Or equivalently,

$$\dot{x}(t) = Ax(t) + Br(t),$$

$$z(t) = Gx(t) + Hr(t), \tag{5}$$

where $x(t) = [q\ \dot{q}]^{\mathrm{T}}$, $r(t)$ and $z(t)$ are the state vector, input vector and output vector, respectively, and

$$A = \begin{bmatrix} 0 & I_9 \\ -M^{-1}K & -M^{-1}C \end{bmatrix}, \quad B = \begin{bmatrix} 0 \\ M^{-1} \end{bmatrix}, \quad G = \begin{bmatrix} I_9 & 0 \\ 0 & I_9 \\ -M^{-1}K & -M^{-1}C \end{bmatrix}, \quad H = \begin{bmatrix} 0 \\ 0 \\ M^{-1} \end{bmatrix},$$

where A, B, G and H are the system matrix, input matrix, output matrix and direct transmission matrix, respectively, $I_{9\times 9}$ is the 9×9 identity matrix, the state variables $x_1, \ldots, x_6$ are the vertical position and pitch angle of carbodies referred to a static equilibrium point, respectively, x_7, x_8, x_9 are the vertical position of bogies referring to a static equilibrium point, respectively, the state variables, $x_{10}, \ldots, x_{18}$ are the time derivative of $x_1, \ldots, x_9$ respectively, $z_1, \ldots, z_{18}$ are the output variables corresponding to $x_1, \ldots, x_{18}$, and the output variables $z_{19}, \ldots, z_{27}$ are the vertical acceleration and angular acceleration of carbodies and the vertical acceleration of bogies, respectively.

4. Problem formulation

The passive suspension parameters are finely tuned, under the practical constraints, to achieve satisfactory ride quality as far as possible. In this passive suspension design study, eight parameters, $c_1, \ldots, c_4$, $k_1, \ldots, k_4$, are to be determined simultaneously.

4.1. Formulation of objectives

The discomfort coefficient is related to the vertical acceleration acting on the passenger. Therefore, the ride quality at each vehicle is defined by directly measuring the accelerations at the gravity centre of the vehicle, at the secondary suspensions mounting, and at the articulation. For a practical suspension design, the following factors should be simultaneously considered: the ride quality due to track irregularity, the primary suspension deflection due to track irregularity, the secondary suspension deflection due to track irregularity, the primary suspension deflection due to track gradient and the secondary suspension deflection due to track gradient. The worst case, i.e. the irregular gradient track, contains the track irregularity and gradient condition. Therefore, the last four factors can be reduced to two, i.e. the primary and secondary deflection due to irregular gradient track.

To conclude the previous observations, it is meaningful to define the averaged r.m.s. acceleration of each vehicle with regard to the random gradient track profiles as the following indexes:

$$J_1 = \sqrt{\frac{1}{3N}\sum_{j=1}^{N}[\ddot{y}_{10}^2(j\tau) + \ddot{y}_1^2(j\tau) + \ddot{y}_{12}^2(j\tau)]}, \tag{6}$$

$$J_2 = \sqrt{\frac{1}{3N}\sum_{j=1}^{N}[\ddot{y}_{13}^2(j\tau) + \ddot{y}_2^2(j\tau) + \ddot{y}_{24}^2(j\tau)]}, \tag{7}$$

$$J_3 = \sqrt{\frac{1}{3N}\sum_{j=1}^{N}[\ddot{y}_{23}^2(j\tau) + \ddot{y}_3^2(j\tau) + \ddot{y}_{11}^2(j\tau)]}, \tag{8}$$

where N is the number of sampling cycles for measuring the related transient signals, and τ is the sampling period. The acceleration of vehicle 2 is taken as the major objective and those of vehicles 1 and 3 are treated as the minor objective.

The suspension travel is composed of static deflection due to the vertical motion of the carbody and bogie, and dynamic deflection due to the load input from irregular gradient tracks. For an irregular gradient track profile, the suspensions must allow movement within the maximum travel range; therefore, six suspension deflections are specified as the constraints:

$$\begin{aligned} g_{11} &= \max_j |y_{10}(j\tau) - y_4(j\tau)|, \quad g_{12} = \max_j |y_4(j\tau) - y_7(j\tau)|, \\ g_{21} &= \max_j |y_2(j\tau) - y_5(j\tau)|, \quad g_{22} = \max_j |y_5(j\tau) - y_8(j\tau)|, \\ g_{31} &= \max_j |y_{11}(j\tau) - y_6(j\tau)|, \quad g_{32} = \max_j |y_6(j\tau) - y_9(j\tau)|. \end{aligned} \tag{9}$$

Larger primary and secondary suspension deflections are, in principle, due to the precipitous track gradients, whereas larger vertical accelerations of the vehicle are owing to the abrupt random tracks. We thus create a random gradient track as the experimental platform to pick up an appropriate combination of the parameter sets $\tilde{c} = [c_1\ c_2\ c_3\ c_4]^{\mathrm{T}}$ and $\tilde{k} = [k_1\ k_2\ k_3\ k_4]^{\mathrm{T}}$.

A three-performance index reflecting the r.m.s. vertical accelerations of the vehicle and ensuring the requirement of ride comfort is investigated. Our objective is to search for an appropriate combination of $\tilde{k}$ and $\tilde{c}$ that makes every objective achieve its optimum while satisfying six constraints imposed on six suspensions. To tackle the issue, we define a minimax problem as follows:

$$\min_{\substack{k_1-k_4,\\ c_1-c_4}} A(\tilde{k},\tilde{c}) \triangleq \min_{\substack{k_1-k_4,\\ c_1-c_4}} \max_{i=1,\dots,3} \frac{J_i(\tilde{k},\tilde{c})}{F_i}, \tag{10}$$

where F_i is the weighting factor with respect to the ith objective function J_i. To broaden the presented approach to cover the general cases of both non-differentiable and differentiable J_i, we approximate $A(\tilde{k},\tilde{c})$ to be a smooth function in the following form [14] as follows:

$$A(\tilde{k},\tilde{c}) \cong \bar{A}(\tilde{k},\tilde{c}), \tag{11}$$

where

$$\bar{A} = \frac{1}{\rho}\ln\left(\sum_{i=1}^{3} \mathrm{e}^{\rho(J_i(\tilde{k},\tilde{c})/F_i)}\right),$$

with the scalar $\rho \gg \ln n$. Through the substitution we may directly adopt the following formulation:

$$\min_{\tilde{k},\tilde{c}} \bar{A}(\tilde{k},\tilde{c}). \tag{12}$$

To employ the searching algorithm the current problem, the control gains must be related to the fitness function $\bar{f}(\tilde{k},\tilde{c})$. Intuitively, we have

$$\bar{f}(\tilde{k},\tilde{c}) \propto \frac{1}{\bar{A}(\tilde{k},\tilde{c})}. \tag{13}$$

A linear equation can be introduced to connect $\bar{A}(\tilde{k},\tilde{c})$ and $\bar{f}(\tilde{k},\tilde{c})$ as follows:

$$\bar{f}(\tilde{k},\tilde{c}) = \lambda \bar{A}(\tilde{k},\tilde{c}) + \zeta, \tag{14}$$

where $\lambda = (\bar{f}_u - \bar{f}_l)/(\bar{A}_l - \bar{A}_u)$ and $\zeta = \bar{f}_u - \lambda \bar{A}_l$ with $\bar{A}_u$ and $\bar{A}_l$ being the largest and smallest values evaluated in the generation, and $\bar{f}_u$ and $\bar{f}_l$ being the corresponding fitness values, respectively.

4.2. Optimization problem with constraints

Constrained optimization deals with the problem of optimizing an objective function in the presence of equality or inequality constraints. The constrained problem provides conditions to criticize the solutions from the solution space. For the current problem, we define a generalized, constrained multiobjective fitness model as follows:

$$\max_{\tilde{k},\tilde{c}} \bar{f}(\tilde{k},\tilde{c}), \tag{15}$$

$$\text{subject to } g_{ij}(\tilde{k},\tilde{c}) \leqslant b_{ij}, \quad i = 1,2,3, \ j = 1,2, \tag{16}$$

where b_{ij} reflects the permissible travel range of suspensions.

The constraints we considered cannot be directly connected to the previously described multiobjective fitness function (15) in the current stage. Consequently, a penalty technique should be imposed to solve the problem. With this technique, the infeasible solutions will be less effective than the feasible ones during the process of selecting the optimal solution. To achieve this goal, we define the following constrained multiobjective fitness function:

$$f(\tilde{k},\tilde{c}) = \bar{f}(\tilde{k},\tilde{c}) p(\tilde{k},\tilde{c}), \tag{17}$$

where the penalty function is defined as

$$p(\tilde{k},\tilde{c}) = 1 - \frac{1}{6} \sum_{i=1}^{2} \sum_{j=1}^{3} \left(\frac{\Delta b_{ij}(\tilde{k},\tilde{c})}{\Delta b_{ij}^{\max}} \right)^{k_{ij}}, \tag{18}$$

$$\Delta b_{ij}(\tilde{k},\tilde{c}) = \max\{0, g_{ij}(\tilde{k},\tilde{c}) - b_{ij}\}, \tag{19}$$

$$\Delta b_{ij}^{\max}(\tilde{k},\tilde{c}) = \max\{\varepsilon, \Delta b_{ij}(\tilde{k},\tilde{c})\}, \tag{20}$$

in which k_{ij} is a modification parameter used to balance the magnitude sensitivity of each term $\Delta b_{ij}/\Delta b_{ij}^{\max}$, $\Delta b_{ij}(\tilde{k}, \tilde{c})$ is the value of violation for the ith constraint, and ε is a small positive number used to have penalty avoid zero-division.

5. EA-based parameter search

The basic element processed by an EA is a vector formed by all k_{ij} and c_{ij}. For the current problem, the population set for w individuals is given by

$$S = \{\underline{k}_1, \underline{k}_2, \ldots, \underline{k}_w\}, \tag{21}$$

where $\underline{k} = [\text{vec}^\text{T} k_1 \ldots \text{vec}^\text{T} k_n \; \text{vec}^\text{T} c_1 \ldots \text{vec}^\text{T} c_n]^\text{T}$, with the 'vec' operator being defined as $\text{vec}\, P = [p_{11} \cdots p_{m1} \vdots p_{12} \cdots p_{m2} \vdots \cdots \vdots p_{1m} \cdots p_{mm}]^\text{T}$ in which $P \in \Re^{m \times m}$.

The idea of ES is to represent an individual as a pair of float-valued vector $v = (\underline{k}_i, N(0, \sigma^2))$ where the first vector $\underline{k}_i$ represents a point in the search space and $N(0, \sigma^2)$ is a vector of independent random Gaussian numbers with zero mean and standard deviation of σ. The search of new points in based on the mutation operator. In (w, λ) ES [7], the search starts by generating w parents in each generation. We choose the number of offsprings $\lambda \gg w$. Then the offsprings are generated by mutation, as a result of the addition of random numbers. Each mutant is subjected to the constraints imposed and the non-feasible one is eliminated. Selection of the qualified mutant is performed until all members are feasible. Next, the λ members are sorted according to the magnitude of the objective function values defined in Eq. (17). Then the w bests of the λ members generated become the parents of the next generation. The offspring (mutant) is accepted as a new member of the population if it has better fitness. Otherwise, the offspring is eliminated, and the original parent remains. Figs. 3 and 4 illustrate the operation of the depicted ES.

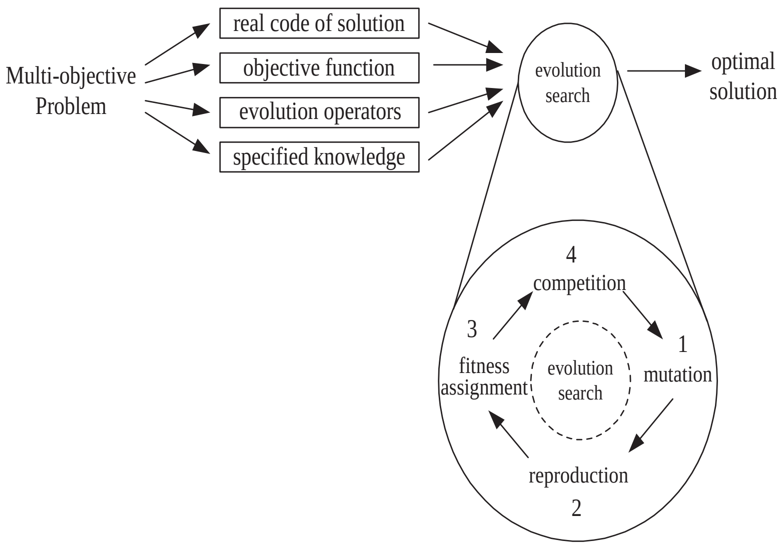

Fig. 3. Operation of EA.

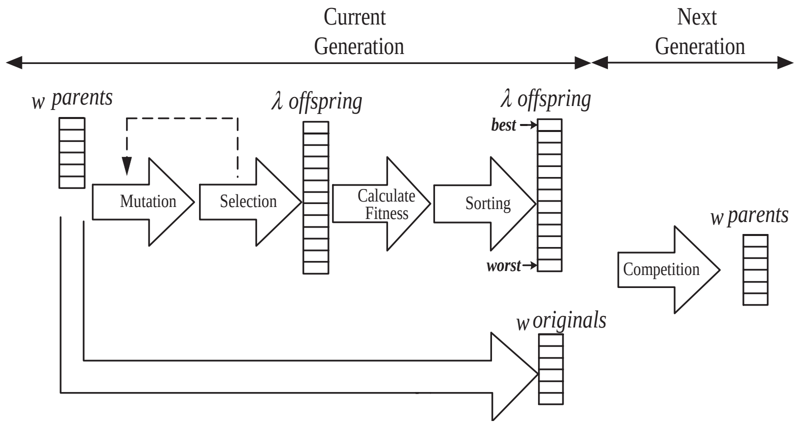

Fig. 4. (w, λ) evolution strategy.

To realize the previous descriptions, we characterize the mutations by replacing the individual $\underline{k}_i$ by

$$\underline{k}_{ij}^{(g+1)} = \underline{k}_{ij}^{(g)} + N(0, \sigma^2), \quad i = 1, \ldots, w, \ j = 1, \ldots, l, \tag{22}$$

where g is the index of the generation number. An appropriate choice of the variable standard deviation σ would speed up the convergence of the evolution searching algorithm to the global minimum of the cost function. A fixed σ may encounter the difficulty that the search cannot escape from the local solution. In contrast, a variable σ makes the search more effective. The process is suggested as follows. Initially, a population of w potential parent solutions $\underline{k}_i, i = 1, \ldots, w$, is chosen based on the selection criterion. Each parent creates an offspring $\underline{k}_i'$, where $\underline{k}_i'$ is determined by the following update criterion:

$$\underline{k}_i' = \underline{k}_i + N(0, \sigma^2), \tag{23}$$

$$\sigma' = \sigma \exp(\zeta), \tag{24}$$

where $\zeta \sim N(0, \Delta\sigma^2)$ is determined according to the normal distribution with zero mean and variance of $\Delta\sigma^2$, in which $\Delta\sigma$ is the difference of σ between the last two generations.

Accordingly, the values of all objective functions and constraints with respect to each offspring are calculated. Each offspring solution $\underline{k}_i'$ is scored in light of the constrained multiobjective fitness function $f(\underline{k})$ where $f(\cdot)$ and $\underline{k}$ are defined, respectively, as in Eqs. (17) and (21).

Each solution $\underline{k}_i'(i = 1, \ldots, \lambda)$ is evaluated against the other randomly chosen solutions from the population. For each comparison, a winner is assigned if the solution's score is higher than, or at least equal to that of its opponent. The w solutions with the greatest number of winners are retained to be parents of the next generation.

The stopping criterion adopted is to terminate the search process when $|f_{\max}^{(g)} - f_{\min}^{(g)}| < \tilde{\varepsilon}$, where $\tilde{\varepsilon}$ is the acceptable upper bound, $f_{\max} = \max_{i=1,\ldots,w} f_i$ and $f_{\min} = \min_{i=1,\ldots,w} f_i$. Otherwise, proceed to generate and examine the next generation. When the stopping criterion is attained, an individual with the highest fitness in the converged population is picked up as the final solution.

6. Results and discussions

Since pure gradient tracks only cause the elongation of suspension system, whereas pure irregular tracks mainly affect the acceleration and reflecting the ride quality, to simplify the analysis and computer burden in the parameter search and incorporate the two kinds of track, only the worst road condition, i.e. the irregular gradient track, is used as the platform for selecting the optimal parameter set. The track is taken to be irregular with one percent gradient and the forward speed $v = 19.4\,\mathrm{m/s}$. The PSD of the track vertical profile is defined by Eq. (1); f is 500 cycle/s; the roughness constant A_1 is 0.00045 in^2 cpf; the break frequencies φ_1 is 0.0071 cpf; and φ_2 is 0.04 cpf.

The duration of computer simulations is set to be 10 s. In the searching procedure of EA, 100 individuals are selected to be the population size for one generation. One hundred generations are executed to validate the convergence of the proposed objective function.

Case 0 (*Nominal parameter design* [15,16]): The passive suspension parameters are designed to pursuit acceptable ride quality, which give a typical power-carbody bounce frequency of 1.24 Hz and a trailer-carbody bounce frequency of 1.37 Hz (with reference to the specification: 1.1–1.4 Hz). The resulting design is listed in Table 1. The allowable stroke and static deflections of the nominal designed suspension are listed in Table 2. The stroke for suspension unit is constrained by the space limitation. From Table 3 we find that the overall acceleration of LRV is $0.3956\,\mathrm{m/s^2}$ (r.m.s.) and the middle car (car 2) has the largest vertical acceleration. For each carbody, acceleration at the end position is larger than that of the centre of gravity due to the pitch effect. It is observed that the total deflections of every suspension are within the allowable limits. Hence, the acceleration can be attenuated further by sacrificing the deflection of suspensions. In the following cases, the EA searching scheme is adopted to search for a

Table 1
Weighting factors and final parameter values obtained for experimental cases

Item	Parameter	Case 0	Case 1	Case 2	Case 3	Case 4
Weighting factor of three vehicles	F_1		1	1	1	1
	F_2		1	0.7	0.2	0.5
	F_3		1	1	1	1
Secondary suspension	k_1 (N/m)	560000	450100	448800	449300	452800
of car 1 and car 3	c_1 (N* s/m)	29584	25200	25300	23800	23800
Secondary suspension	k_2 (N/m)	1092000	892100	876700	877500	878800
of car 2	c_2 (N* s/m)	50205	41200	42600	41200	40200
Primary suspension	k_3 (N/m)	2400000	2696100	2845900	2772900	2107900
of car 1 and car 3	c_3 (N* s/m)	11883	13600	12800	12700	13700
Primary suspension	k_4 (N/m)	3864000	3652600	3289100	4476400	3388000
of car 2	c_4 (N* s/m)	176673	184400	176200	179400	204500

F_i: weighting factor of the ith car.

Table 2
Maximal suspension deflections on random gradient track (mm)

Item	Deflection	Case 0	Case 1	Case 2	Case 3	Case 4	Allowable
Static deflection							
Suspension of car 1	y_4–y_7	42.0435	37.4261	35.4561	36.3895	47.8697	
	y_{10}–y_4	128.737	160.1699	160.6338	160.4551	159.2148	
Suspension of car 2	y_5–y_8	31.8227	33.6645	37.3850	37.4692	36.2937	
	y_2–y_5	102.283	125.2024	127.4017	127.2856	127.0973	
Suspension of car 3	y_6–y_9	42.0435	37.4261	35.4561	36.3895	47.8697	
	y_{11}–y_6	128.737	160.1699	160.6338	160.4551	159.2148	
Dynamic deflection							
Suspension of car 1	y_4–y_7	2.1041	2.0112	1.9923	2.0084	2.1493	
	y_{10}–y_4	3.4265	3.7831	3.7598	3.8996	4.0103	
Suspension of car 2	y_5–y_8	1.8015	1.7837	1.7938	1.7660	1.7808	
	y_2–y_5	1.8783	1.9605	1.9301	2.0006	1.8732	
Suspension of car 3	y_6–y_9	2.1300	2.0412	2.0236	2.0428	2.1715	
	y_{11}–y_6	3.4617	3.7948	3.7596	3.9318	4.0094	
Total deflection							
Suspension of car 1	y_4–y_7	44.1476	39.4373	37.4484	38.3976	50.0189	55
	y_{10}–y_4	132.1630	163.9530	164.3937	164.3546	163.2251	165
Suspension of car 2	y_5–y_8	33.6242	35.4482	39.1788	39.2352	38.0745	40
	y_2–y_5	104.1614	127.1629	129.3318	129.2861	128.9705	130
Suspension of car 3	y_6–y_9	44.1735	39.4673	37.4797	38.4324	50.0411	55
	y_{11}–y_6	123.1982	163.9646	164.3935	164.3869	163.2242	165

Table 3
Ride quality on the random track (m/s^2)

Item	Vertical acceleration	Case 0	Case 1	Case 2	Case 3	Case 4
On track						
Acceleration of car 1	$\ddot{y}_{10}$	0.3981	0.3828	0.3819	0.3888	0.3972
	$\ddot{y}_1$	0.2444	0.2214	0.2205	0.2248	0.2259
	$\ddot{y}_{12}$	0.4927	0.4447	0.4435	0.4529	0.4294
Acceleration of car 2	$\ddot{y}_{13}$	0.4275	0.3911	0.3900	0.3979	0.3795
	$\ddot{y}_2$	0.3903	0.3363	0.3342	0.3429	0.3219
	$\ddot{y}_{24}$	0.4267	0.3878	0.3882	0.3960	0.3721
Acceleration of car 3	$\ddot{y}_{23}$	0.4820	0.4214	0.4193	0.4316	0.4097
	$\ddot{y}_3$	0.2397	0.2319	0.2311	0.2358	0.2335
	$\ddot{y}_{11}$	0.3745	0.3727	0.3705	0.3817	0.3884
Objective function	J1	0.3920	0.3621	0.3611	0.3682	0.3620
of car 1, car 2 and car 3	J2	0.4152	0.3726	0.3717	0.3798	0.3588
	J3	0.3786	0.3513	0.3495	0.3594	0.3527
Overall LRV	$f(\tilde{k}, \tilde{c})$	0.3956	0.3621	0.3609	0.3692	0.3578

$$\ddot{y}_{irms} = \sqrt{\frac{1}{N}\sum_{j=1}^{N} \ddot{y}_i^2(\mathrm{j}\tau)}, \quad T = 10\ (\mathrm{s}).$$

better solution which may improve the ride quality and compromise with the deflection of suspensions.

Case 1: The passive suspension parameters are restricted within the range from 80% to 120% of their nominal values set in Case 0 to examine the ride quality and check if the natural frequency of carbodies still meets the specification. The weighting factors F_1, F_2, and F_3 are equally set. This means that we are equally concerned with the ride quality of three cars. From Table 3, we find that the overall acceleration reduces to $0.3621\,\mathrm{m/s^2}$ (r.m.s.). However, this result only presents a slight improvement in the ride quality. Hence, it is necessary to assign different weighting factors for three cars to make the necessary trade-off on the individual ride quality.

Case 2: In case 2, the passive suspension parameters are also restricted within the range from 80% to 120% of their nominal values. The weighting factors F_1, F_2, and F_3 are set to be 1, 0.7, and 1, respectively. This means that the ride quality of the middle car is of major concern. In Table 3, we find that the overall acceleration reduces to $0.3609\,\mathrm{m/s^2}$ (r.m.s.). This result presents only a slightly better ride quality.

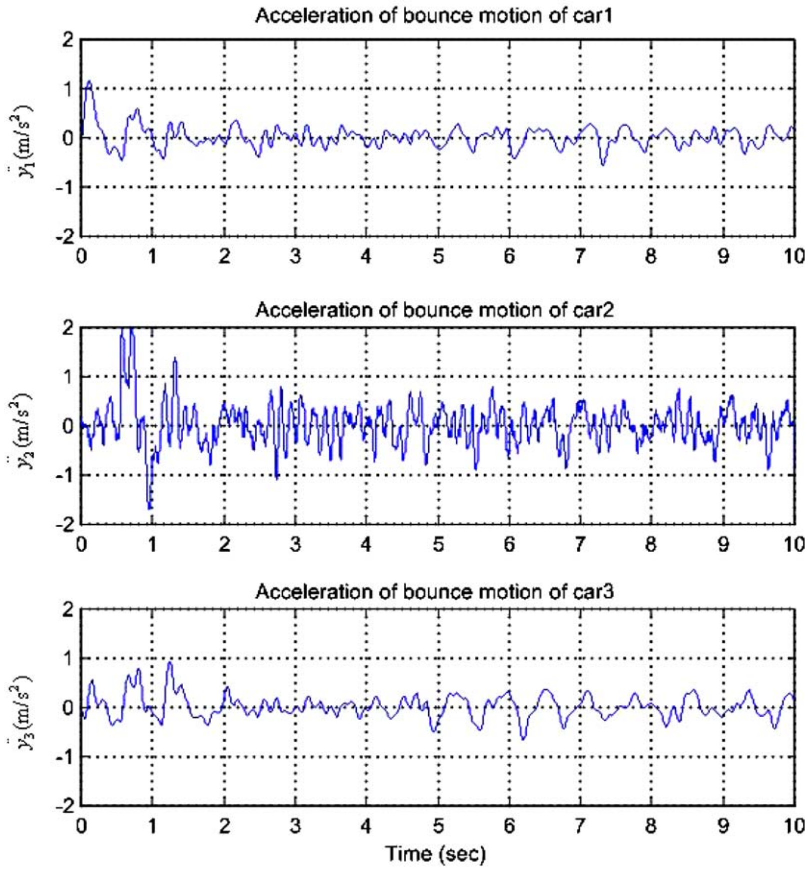

Fig. 5. Acceleration of the bounce motion.

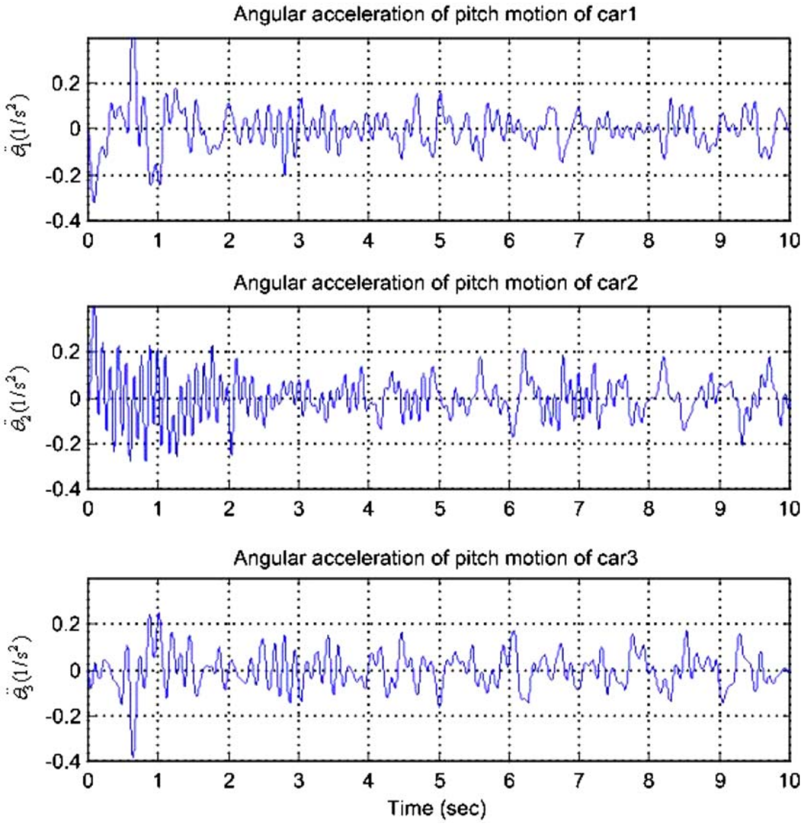

Fig. 6. Angular acceleration of the pitch motion.

Case 3: The passive suspension parameters are kept invariant as those in the previous cases. The weighting factors F_1, F_2, and F_3 are set to be 1, 0.2, and 1, respectively. The overall acceleration increases to $0.3692\,\mathrm{m/s^2}$ (r.m.s.).

Case 4: The weighting factors F_1, F_2, and F_3 are set to be 1, 0.5, and 1, respectively. From Table 3, the overall acceleration of LRV reduces to $0.3578\,\mathrm{m/s^2}$ (r.m.s.). Consequently, the ride quality is significantly improved by 9.56%. Obviously, all deflections of the suspensions are enlarged and within the allowable values. The new passive suspension parameter set gives the power-carbody bounce frequency of 1.16 Hz and the trailer-carbody bounce frequency of 1.28 Hz. Figs. 5–7 illustrate the major transient responses of the centre of gravity of carbodies. Deflections of all suspensions due to the irregular gradient track are exhibited in Fig. 7.

The convergence of the objective function of evolution search is demonstrated in Fig. 8. For comparison, the fitness value convergence of the binary coded GA with the same scenario setting is illustrated in Fig. 9. It is seen that the EA converges in 65 generations, whereas the GA did not attain steady after 100 generations. This shows the excellent efficiency of the proposed EA.

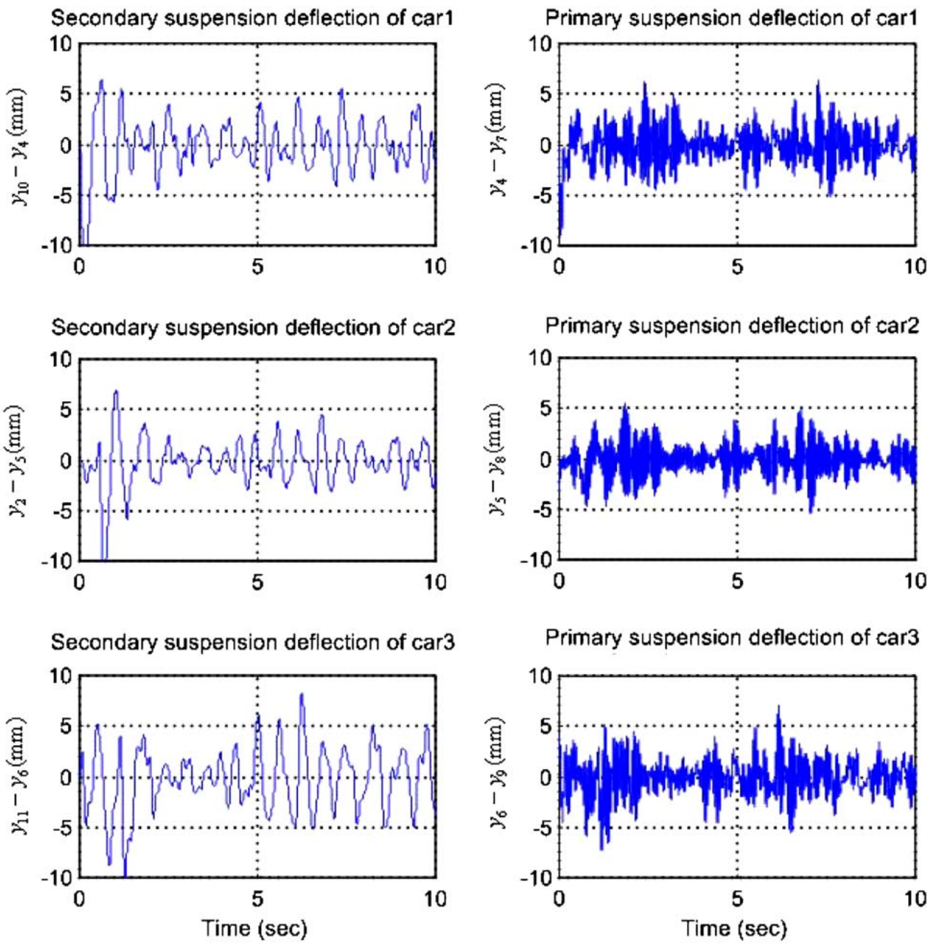

Fig. 7. Suspension deflections due to irregular gradient track.

7. Conclusions

A systematic and effective optimization scheme for the design of vertical passive suspension of an LRV by applying constrained multiobjective evolution algorithms is proposed. The multibody dynamic model together with the proposed searching procedure makes it possible to optimize all suspension spring and damping parameters even for a complex dynamics application such as the LRV. We show that the proposed design is able to offer satisfactory ride quality while maintaining the suspension deflections within the allowable levels on irregular gradient tracks. It is further found that if the allowable workspace of suspension is expanded, the weighting factors in objective function can be correspondingly modified to obtain different sets of suspension parameters improving the ride quality.

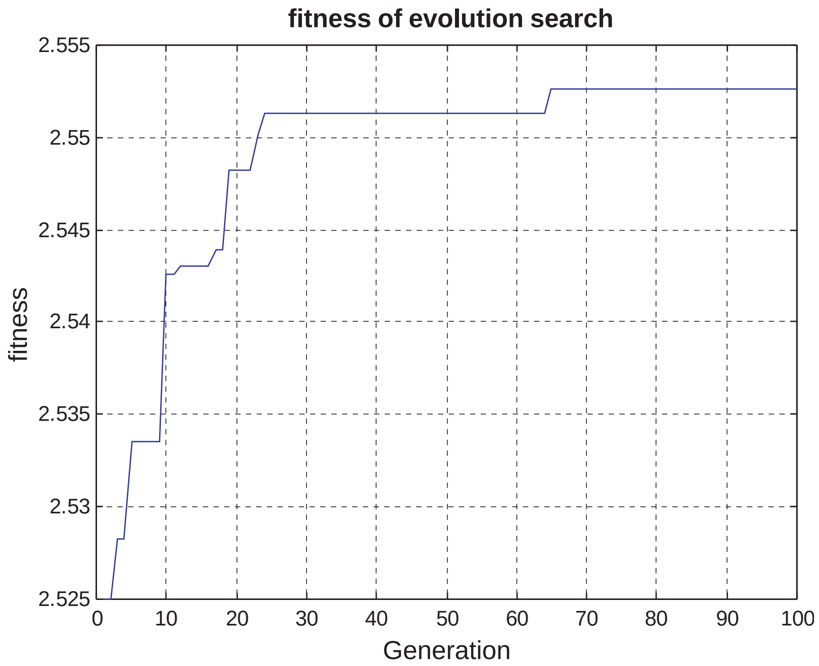

Fig. 8. Convergence of the fitness value using the EA.

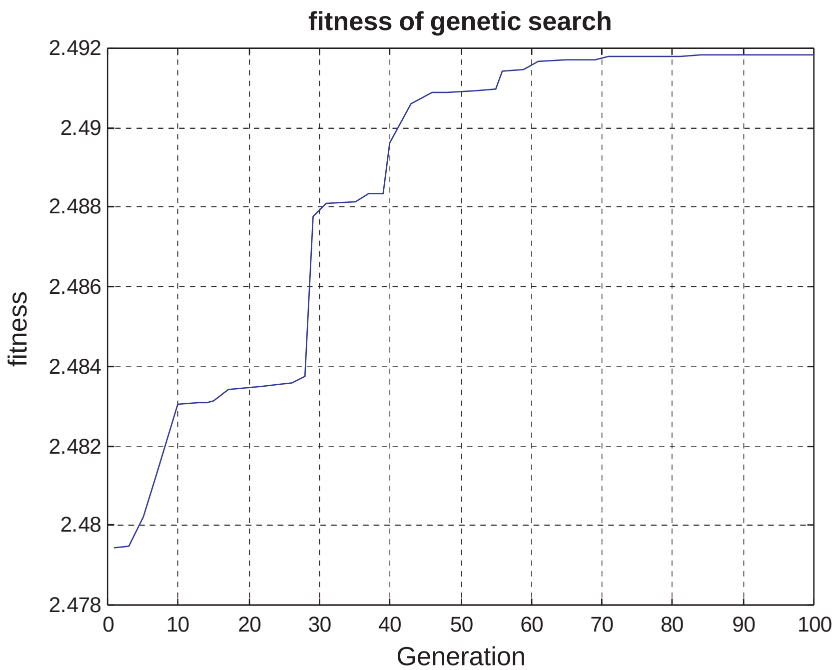

Fig. 9. Convergence of the fitness value using a GA.

Acknowledgements

The work presented is a part of a research project sponsored by Ministry of Economics, Taiwan, ROC and Chung Shan Institute of Science and Technology, Taiwan, ROC, under the contract 92-EC-2-A-17-0150-19.

References

[1] G. Mastinu, A method to design optimal railway vehicles, in: *Proceedings of World Congress of Railway Research*, Florence, 1997.
[2] T.X. Mei, R.M. Goodall, Use of multiobjective genetic algorithms to optimize inter-vehicle active suspensions, *Journal of Rail and Rapid Transit* 216 (2002) 53–63.
[3] G.R.M. Mastinu, M. Gobbi, On the optimal design of railway passenger vehicles, *Journal of Rail and Rapid Transit* 215 (2001) 111–124.
[4] H. Li, R.M. Goodall, Linear and non-linear skyhook damping control laws for active railway suspensions, *Control Engineering Practice* 7 (1999) 843–850.
[5] C.L. Lin, H.Y. Jan, N.C. Shieh, GA-based multiobjective PID control for a linear brushless DC motor, *IEEE/ASME Transactions on Mechatronics* 8 (2003) 56–65.
[6] T. Bäck, *Evolutionary Algorithms in Theory and Practice*, Oxford University Press, New York, 1996.
[7] H.P. Schwefel, *Evolution and Optimum Seeking*, Wiley, New York, 1995.
[8] L. Costa, P. Oliveira, Evolutionary algorithms approach to the solution of mixed integer non-linear programming problems, *Computers and Chemical Engineering* 25 (2001) 257–266.
[9] D.E. Goldberg, *Genetic Algorithms in Search, Optimization, and Machine Learning*, Addison-Wesley, Reading, MA, 1989.
[10] M. Gen, R. Cheng, A survey of penalty techniques in genetic algorithms, in: *Proceedings of IEEE International Conference on Evolutionary Computation*, Nagoya, Japan, 1996, pp. 804–809.
[11] V.K. Garg, R.V. Dukkipati, *Dynamics of Railway Vehicle Systems*, Academic Press, New York, 1984.
[12] J.S. Bendat, A.G. Piersol, *Random Data: Analysis and Measurement Procedures*, Wiley, New York, 1986.
[13] R.R. Craig, *Structural Dynamics*, Wiley, New York, 1981.
[14] J.M. Maciejowski, *Multivariable Feedback Design*, Addison-Wesley, New York, 1989.
[15] H. Albrecht, K. Albrecht, K. Bader, E. Breiding, K.D. Breuer, H. Fiedler, W.F. Baldenius, P. Forcher, R. Frank, G. Hutschenreuter, S. Muller, U. Stahlberg, G. Steller, Recommendation of type-light rail vehicles, VDV Recommendation 150, 1996.
[16] H. Bugarcic, L. Geers, E.M. Plate, Structural requirements to rail vehicles for the public mass transit in accordance with BOStrab, VDV Recommendation 152, 1992.